



DATA NOTE

# The 'ALSPAC in London' dataset: adiposity, cardiometabolic risk profiles, and the emerging arterial phenotype in young adulthood [version 1; referees: awaiting peer review]

Scott T. Chiesa <sup>1</sup>, Alicja Rapala<sup>1,2</sup>, Marietta Charakida<sup>1,3</sup>, Kaitlin H. Wade<sup>4,5</sup>,  
Nicholas J. Timpson <sup>4,5</sup>, John E. Deanfield<sup>1</sup>

<sup>1</sup>Vascular Physiology Unit, UCL Institute of Cardiovascular Science, London, UK

<sup>2</sup>Department of Population Science and Experimental Medicine, UCL Institute of Cardiovascular Science, London, UK

<sup>3</sup>Division of Imaging Sciences and Biomedical Engineering, King's College London, London, UK

<sup>4</sup>Population Health Sciences, Bristol Medical School, University of Bristol, Bristol, UK

<sup>5</sup>MRC Integrative Epidemiology Unit, University of Bristol, Bristol, UK

**v1** First published: 23 Dec 2018, 3:162 (<https://doi.org/10.12688/wellcomeopenres.14942.1>)

Latest published: 23 Dec 2018, 3:162 (<https://doi.org/10.12688/wellcomeopenres.14942.1>)

## Abstract

Rising rates of adiposity in the young pose one of the greatest threats to future population burden of cardiovascular disease. Understanding the contribution of genetic and early-life influences to adiposity profiles in young adulthood – when the first signs of subclinical cardiovascular disease commonly appear – are vital if effective lifetime prevention strategies are to be developed. This data note documents the extensive range of genotypic and phenotypic data available from a London-based sub-study of the long-running Avon Longitudinal Study of Parents and Children (ALSPAC)—the 'ALSPAC in London' Study—in which extensive adipose and cardiovascular phenotyping was carried out in participants recruited based on a genetic predisposition to obesity.

## Keywords

Adiposity, cardiometabolic risk, arterial phenotypes, ALSPAC

## Open Peer Review

**Referee Status:** *AWAITING PEER*

*REVIEW*

## Discuss this article

Comments (0)



This article is included in the [Avon Longitudinal Study of Parents and Children \(ALSPAC\)](#) gateway.

**Corresponding author:** Scott T. Chiesa ([s.chiesa@ucl.ac.uk](mailto:s.chiesa@ucl.ac.uk))

**Author roles:** **Chiesa ST:** Conceptualization, Data Curation, Methodology, Project Administration, Writing – Original Draft Preparation; **Rapala A:** Conceptualization, Data Curation, Methodology, Project Administration, Writing – Review & Editing; **Charakida M:** Conceptualization, Data Curation, Methodology, Writing – Review & Editing; **Wade KH:** Conceptualization, Methodology, Writing – Review & Editing; **Timpson NJ:** Conceptualization, Funding Acquisition, Methodology, Resources, Supervision, Writing – Review & Editing; **Deanfield JE:** Conceptualization, Funding Acquisition, Resources, Supervision, Writing – Review & Editing

**Competing interests:** No competing interests were disclosed.

**Grant information:** This publication is the work of the authors and STC will serve as guarantor for the contents of this paper. The UK Medical Research Council and Wellcome Trust (Grant ref: 102215/2/13/2) and the University of Bristol provide core support for ALSPAC. This research was specifically funded by the British Heart Foundation (BHF Programme Grant No. RG/10/004/28240). JED was a BHF-funded Professor during the time of this study. NJT is a Wellcome Trust Investigator (202802/Z/16/Z), is the PI of the Avon Longitudinal Study of Parents and Children (MRC & WT 102215/2/13/2), is supported by the University of Bristol NIHR Biomedical Research Centre (BRC-1215-20011), the MRC Integrative Epidemiology Unit (MC\_UU\_12013/3) and works within the CRUK Integrative Cancer Epidemiology Programme (C18281/A19169). KHW was supported by a Wellcome Trust Grant (096989/Z11/Z). A comprehensive list of grants funding is available on the ALSPAC website.

*The funders had no role in study design, data collection and analysis, decision to publish, or preparation of the manuscript.*

**Copyright:** © 2018 Chiesa ST *et al.* This is an open access article distributed under the terms of the [Creative Commons Attribution Licence](https://creativecommons.org/licenses/by/4.0/), which permits unrestricted use, distribution, and reproduction in any medium, provided the original work is properly cited.

**How to cite this article:** Chiesa ST, Rapala A, Charakida M *et al.* **The ‘ALSPAC in London’ dataset: adiposity, cardiometabolic risk profiles, and the emerging arterial phenotype in young adulthood [version 1; referees: awaiting peer review]** Wellcome Open Research 2018, 3 :162 (<https://doi.org/10.12688/wellcomeopenres.14942.1>)

**First published:** 23 Dec 2018, 3:162 (<https://doi.org/10.12688/wellcomeopenres.14942.1>)

## Introduction

The recent worldwide increase in population adiposity threatens to reverse achieved reductions in cardiovascular morbidity and mortality. The fastest rises in adiposity rates have been in children, teenagers and young adults and therefore represent one of the major growing threats to worldwide public health. The Avon Longitudinal Study of Parents and Children (ALSPAC) is a longitudinal birth cohort that recruited pregnant women living near Bristol, UK with an estimated delivery date between 1991 and 1992. The study includes extensive phenotypic, genetic, epigenetic and metabolomic data on the mothers, fathers and children from questionnaires, clinics and samples, and follow up is ongoing. Using a novel ‘recall-by-genotype’ study design to identify individuals with genetically predicted variation in body mass index (BMI)<sup>1</sup>, the ‘ALSPAC in London’ study aimed to examine the impact of adiposity on metabolic, inflammatory and autonomic disturbances, as well as their relationship to cardiovascular (CV) structure and function, with genetically-directed deep phenotyping.

## Methods

ALSPAC recruited 14,541 pregnant women resident in Avon, UK (former county covering Bristol and the surrounding areas in the South West UK) with expected dates of delivery 1st April 1991 to 31st December 1992<sup>2,3</sup>. The initial number of pregnancies for which the mother enrolled in the ALSPAC study and had either returned at least one questionnaire or attended a “Children in Focus” clinic by 19/07/99 is 14,541. Of these initial pregnancies, there were a total of 14,676 fetuses, resulting in 14,062 live births and 13,988 children who were alive at 1 year of age. When the oldest children were approximately 7 years of age, an attempt was made to bolster the initial sample with eligible cases who had failed to join the study originally. As a result, when considering variables collected from the age of seven onwards (and potentially abstracted from obstetric notes) there are data available for more than the 14,541 pregnancies mentioned above.

The number of new pregnancies not in the initial sample (known as Phase I enrolment) that are currently represented in the study and reflecting enrolment status at the age of 18 is 706 (452 and 254 recruited during Phases II and III respectively), resulting in an additional 713 children being enrolled. The phases of enrolment are described in more detail in the cohort profile paper<sup>2,3</sup>.

The total sample size for analyses using any data collected after the age of seven is therefore 15,247 pregnancies, resulting in 15,458 fetuses. Of this total sample of 15,458 fetuses, 14,775 were live births and 14,701 were alive at 1 year of age<sup>2,3</sup>.

The data included in this resource were collected from 436 young adults (mean age  $21 \pm 1$  years) recalled for extensive adipose and cardiometabolic phenotyping between 2011 and 2015. Of these, 419 were recruited based on a genetic propensity for high or low BMI, with the other 17 comprising

patients recruited prior to the decision to employ a recall-by-genotype study design.

## Dataset 1 – genetic risk groups

Original beta-coefficients for the genome-wide genetic risk score (GRS) assembly were obtained directly from the genome-wide association study (GWAS) of BMI, conducted in 2010 by Speliotes *et al.*<sup>4</sup>, with the ALSPAC data removed from the release. All alleles were aligned such that the reference allele matched the BMI-increasing direction reported in the GWAS and plink (--score) was used to derive a score for each participant (N=8,350). After removing heterozygous haploid genotypes (N=46,067), direct genotypes were available for 500,527 SNPs, of which 472,208 mapped to SNPs that overlapped with the Speliotes *et al.*<sup>4</sup> GWAS results and 470,667 mapped to alleles. The ALSPAC genetic dataset used was the best available data at the time of the RbG study design (2012) and was subsequently used in several papers<sup>5,6</sup>. The number of participants invited and recruited to the RbG study was orchestrated based on an *a priori* power calculation taking into account the predicted explained variation in BMI by the genome-wide GRS and its effect size on an example cardiovascular phenotype (SBP). Specifically, using the observed association between SBP and BMI at age 17, we calculated that we would require 450 participants in our RbG to be able to detect a difference of 3 mmHg (a difference that in young adulthood has clinically meaningful association with future cardiovascular disease (CVD)<sup>7</sup> with 80% power and a two-sided p-value threshold of 0.05 and assuming an approximate 3.3kg/m<sup>2</sup> unit difference in BMI between recalled groups. Participants were then recruited according to their appearance in nine sampling groups, from the most extreme to the least, to maximise power and difference in BMI. These samples were as follows: 3%, 6%, 9%, 12%, 15%, 18%, 21%, 24%, 27% from the lower tail of the genome-wide GRS distribution and 97%, 94%, 91%, 88%, 85%, 82%, 79%, 76%, 73% from the upper tail of the genome-wide GRS distribution. The GRS was computed for 4,602 individuals in total within these sampling groups. Of those who were invited to the study (N=2,071), 419 individuals attended from across the entire distribution of sampling groups and had both full genetic and BMI data.

## Dataset 2 – participant characteristics

Height was measured in metres using a stadiometer (SECA 213, Birmingham, UK) and weight in kilograms using electronic weighing scales (Marsden M-110, Rotherham, UK). BMI was calculated as weight (kg) / height (m)<sup>2</sup>. Waist circumference was measured in centimetres at the narrowest circumference of the abdomen (roughly level to the umbilicus) using a standard flexible tape measure. Hip circumference was measured in centimetres at the widest circumference of the hips/buttocks using a standard flexible tape measure. Sagittal abdominal diameter was measured in centimetres as the distance between the small of the back and the top of the abdomen, with all measurements taken in the supine position with specialist metal callipers. Numerous other measures such as medical history, recent

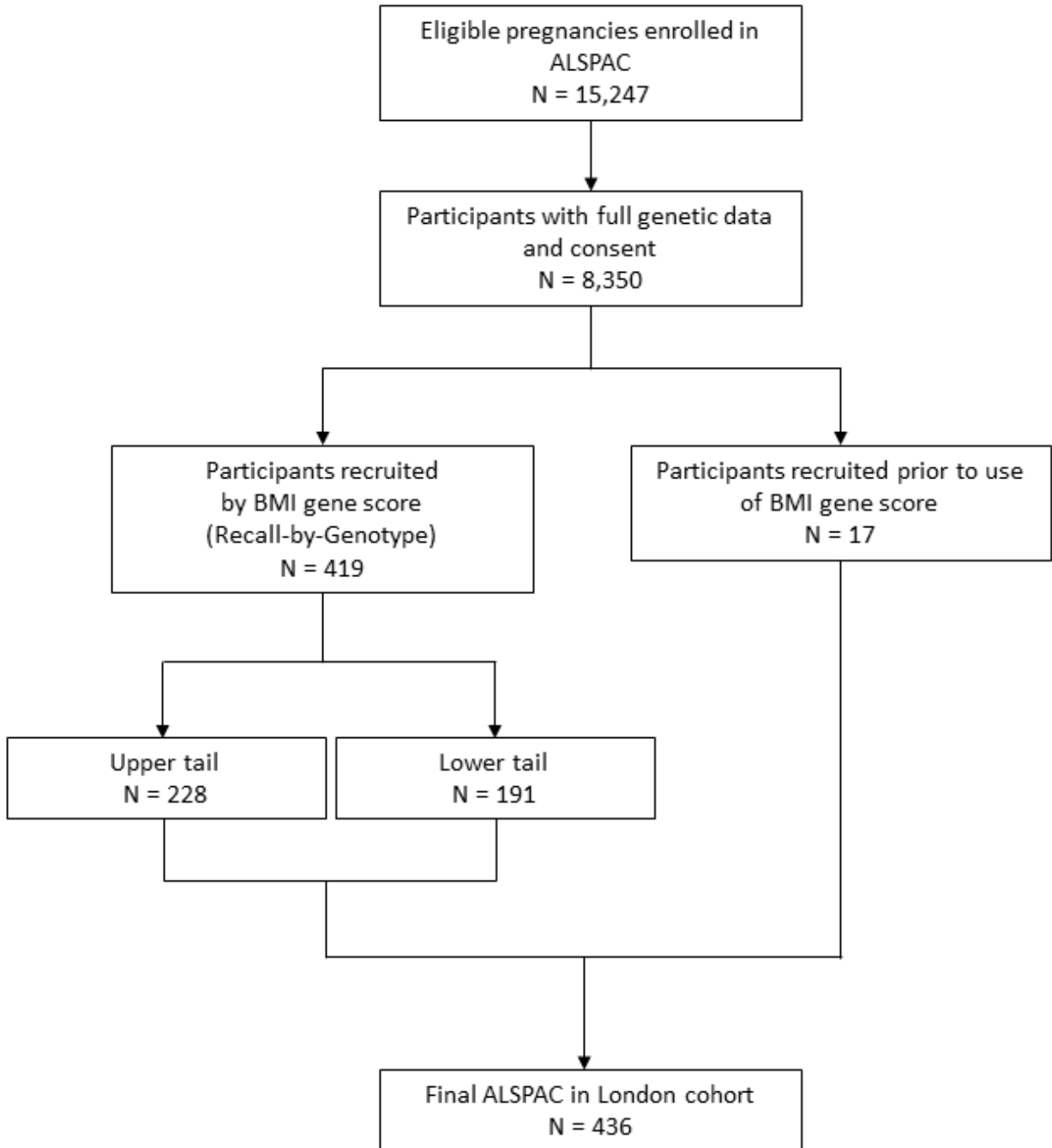


**Figure 1. Study flow diagram.**

illnesses, smoking, alcohol consumption, physical activity and menstrual cycle were recorded via questionnaire, a copy of which is available as extended data<sup>8</sup>.

#### Dataset 3 – adipose phenotypes

Body fat volume and distribution was measured using a 1.5T magnetic resonance imaging (MRI) system (Avanto; Siemens Medical Solutions). A graphics processing unit (GPU) implementation of the T2-IDEAL algorithm was used to measure body

fat content. This technique iteratively separated MR images into fat and water components, which could then be used to measure the proportion of fat in each 36x36x10 mm voxel. Data was acquired in a continuous stack of 10 mm thick slices from the neck to the knees. To prevent motion artefact, breath holding was used for the thorax and abdomen and cardiac gating for slices containing the heart. Fat quantification in the head, arms and below the knees was impractical due to the need for participant re-positioning or specialised coils. Due to their low fat content

these body parts were excluded using anatomical landmarks to ensure consistency between participants. The visceral compartment was manually separated from the fat image and the liver was excluded due to frequent artefacts at diaphragm level. Absolute volumes of fat were calculated for subcutaneous, visceral, liver, and pericardial deposits.

#### Dataset 4 – cardiovascular phenotypes

**Carotid intima-media thickness.** Common carotid artery intima-media thickness (cIMT) was measured using B-mode ultrasound images acquired in the ear-to-ear plane with the head rotated to 45° from the midpoint using a Zonare Z.OneUltra system equipped with a L10-5 linear transducer (Zonare Medical Systems, CA, US). Images were recorded in Digital 2 Imaging and Communications in Medicine (DICOM) format as 10 second cine-loop files for offline analysis using Carotid Analyzer software (Medical Imaging Applications, Coralville, IA). Left and right cIMT were taken to be the average of three end-diastolic measurements located on the far-wall of a single segment of arterial wall 5–10 mm in length and 10 mm proximal to the bifurcation.

**Pulse wave velocity.** Pulse-wave velocity (PWV) was used to estimate arterial stiffness via applanation tonometry (SphygmoCor Vx, AtCor Medical, NSW, Australia). Two distinct indices of PWV were measured, using electrocardiogram (ECG)-gated pulse waves travelling between both carotid-radial and carotid-femoral sites. The participant was rested in a supine position and a handheld tonometer was placed over the left carotid artery in order to allow the recording of 10–12 clear and reproducible pressure waveforms. The same tonometer was then used to measure a similar number of femoral arterial pulse waveforms in the inguinal crease at the top of the right leg, or radial arterial pulse waveforms in the right wrist. Carotid-radial transit distance was measured between the upper edge of the suprasternal notch and the radial pulse measurement site using a tape measure, whereas carotid-femoral transit distance was measured between carotid and femoral sites both directly and via the umbilicus. The device software calculated the mean transit time (in milliseconds) from the recorded pulse waveforms and carotid-femoral and carotid-radial PWV were calculated as the transit distance/transit time.

**Pulse wave analysis.** Estimates of central blood pressure (BP) and indices of systemic arterial stiffness such as augmentation pressure (AP) and augmentation index (AIx) were assessed using pulse wave analysis (SphygmoCor Vx, AtCor Medical, NSW, Australia). This technique measures the arterial pressure waveform at the radial artery and applies a validated generalised transfer function to provide the central pressure waveform. Participants lay supine on a couch in ambient conditions for at least 10 mins prior to the start of the assessment. Brachial BP was measured using a digital automated sphygmomanometer (Omron M6 Comfort). With the participant's wrist held steady, the tonometer probe was placed over the right radial artery at the level of the wrist and a recording of 10–12 pressure waveforms was saved to specialist software. Quality indices (average pulse height, pulse height variation, diastolic variation, and shape deviation) were

assessed for each measurement to confirm they fell within acceptable limits (automatically calculated), otherwise the scan was repeated.

**Autonomic function.** Autonomic function was assessed using measures of baroreflex sensitivity (BRS) and heart rate variability (HRV). Participants lay supine on a couch in a darkened room in ambient conditions for at least 10 mins prior to the start of the assessment. Following this, a 3-lead ECG and 4-lead respiratory monitoring system were attached to the participant's chest to measure heart rate and breathing cycle, while an inflatable infrared photoplethysmographic cuff (Portapres, FMS, Netherlands) was attached to the middle finger of the right hand and (following calibration) inflated in order to continuously and non-invasively measure BP. Participants remained at rest for 20 mins while measurements were recorded by the software, with all signals fed to specialist software for the calculation of BRS and HRV. A stationary period of 5 min with less than 5% atrial/ventricular ectopic beats was chosen for the temporal QT interval variability analysis using a computer algorithm. The examiner defined a template QT interval for one beat from the beginning of the QRS complex to the end of T wave, including all deflections that might relate to repolarization, including possible U waves. The algorithm found the QT intervals of all other beats by determining the stretch or compression in time of each beat that best matched the ST segment and the T wave of the template beat, whereas the QRS complex was ignored. RR interval mean and variance and QT interval mean and variance were derived from the respective time series. QTVI, which represents the log ratio between normalized QT and RR interval variability, was calculated according to the equation:  $QTVI = \log_{10} [(QTv / QTm^2) / (RRv / RRm^2)]$ , whereby a difference of 1 QTVI between two individuals implies a tenfold difference in temporal QT variability normalized to the QT interval, RR variance (HRV calculated in the time domain) and the RR interval. The squared coherence function was calculated from power spectra of the RR and QT interval time series and the cross-spectrum between these two series derived by fast Fourier Transform (Welch algorithm, five blocks, 50% overlap, Hanning window). The mean squared coherence was obtained by averaging the coherence function over the frequency band from 0 to 0.45 Hz. The coherence provides a measurement of the degree of linear interaction between the RR and QT interval fluctuations as a function of the frequency of those fluctuations. For BRS calculations, registrations were recorded at a sampling frequency of 1000 Hz and stored on a computer. The recordings were inspected offline for the removal of artefactual segments and sequences containing non-sinus beats. Ectopic beats were corrected by interpolation. The time series of systolic blood pressure (SBP) and RR interval from the entire period of recording (20 min) were scanned to identify baroreflex sequences, which were defined as three or more consecutive beats in which successive SBP and RR intervals concordantly increased or decreased, with the threshold set at 1.0 mmHg and 5.0 ms, respectively, and a shift of +1 between the BP pulse and the RR interval, resembling the classical criteria suggested by Bertinieri *et al.*<sup>9</sup> (threshold values of 1.0 mmHg and 4.0 ms, respectively and shift 1). Linear regression was applied to each sequence and only those for

which the square of the correlation coefficient ( $r^2$ ) was greater than 0.85 were accepted for further analysis. The spontaneous BRS was calculated, reflecting the average regression slope for all the linear regressions. RR data were used to derive standard deviation of normal-to-normal RR intervals (SDNN) for time-domain HRV.

**Ultra-high frequency ultrasound (UHFUS).** In a randomly-selected sub-sample of participants, images of individual intima and media thicknesses (IT and MT, respectively) were obtained in the carotid, radial and dorsal pedal arteries using an ultra-high resolution ultrasound system (UHFUS; Vevo 2100, Visualsonics) with attached 40 MHz and 50 MHz transducers. Right common carotid artery scans were obtained via UHFUS and imaged longitudinally 1–2 cm proximal to the carotid bifurcation. Images were focused on the posterior (far) wall of the artery and the zoom function was used to magnify the area. Right radial artery scans were collected in the same way at a location 1–2 cm proximal to the skin fold separating the palma manus from the region antebrachii anterior. Right dorsal pedal scans were measured above the proximal first metatarsal bone in the foot. Images were recorded in DICOM format as cine loops for off-line analysis. IT echo was assessed offline and its total thickness measured with callipers within a standardised (8mm×8 mm) higher resolution zoom. The image was acquired, temporarily stored in the cine loop and consecutively zoomed when the measurements were done. The measurements of the IT were performed in systole of the vessel (determined by scrolling through the cine loop to reach the arteries largest diameter). The MT was then calculated as the difference between IMT and IT ( $MT = IMT - IT$ ). IMT was defined as the distance from the leading edge of the lumen–intima interface to the leading edge of the media–adventitia interface. Lumen diameter was defined by the distance between the leading edges of the intima–lumen interface of the near wall and the lumen–intima interface of the far wall.

**Cardiovascular magnetic resonance imaging.** Cardiovascular MRI was used to assess numerous measures of cardiovascular structure and function. All measures were made using a 1.5T MR scanner (Avanto, Siemens Medical Solutions, Erlangen, Germany). Endocardial borders of the left ventricle (LV) were traced manually on short axis stacks at end-diastole and end-systole to evaluate end-diastolic volume (EDV) and end-systolic volume (ESV). Stroke volume (SV) was obtained by subtracting ESV from EDV. Epicardial borders were traced in end-diastole to calculate an epicardial volume. The EDV was subtracted from this volume, multiplied by assumed myocardial density to obtain left ventricular mass (LVM). Flow quantification was performed through-plane in a cross-section of the ascending aorta as it passes the bifurcation of the pulmonary arteries using an ECG-gated spiral phase-contrast MRI sequence. This technique allows images to be acquired within a short breath-hold (0.5 seconds) with a spatial resolution of 1.6 x 1.6 mm and a temporal resolution of 30 ms. All images were processed using in-house plug-ins for the Open source software OsiriX (OsiriX Foundation, Geneva, Switzerland). Flow images were manually segmented (using the modulus images) and SV (ml) was measured

and cardiac output (CO, L/min) calculated as  $SV \times \text{heart rate}$ . At the time of flow imaging, BP was simultaneously measured using MRI-compatible oscillometric sphygmomanometer (Datex Ohmeda). Systemic vascular resistance (SVR; measured in mmHg/L/min) was calculated by dividing the measured mean BP by CO. Total arterial compliance (TAC) was calculated by optimisation of the two-element Windkessel model. Briefly, the flow curves and SVR were used as inputs to the model. Pulse pressure (PP) was calculated for a series of modelled pressure curves generated using a range of TAC values from 0.1 to 5.0 mL/mmHg in increments of 0.01. The compliance value that gave the smallest error between the modelled PP and the true PP was taken to be the true compliance.

#### Dataset 5 – metabolic/metabolomic phenotypes

In order to assess cardiometabolic risk profiles, 15 ml of blood was collected at least 4–6 h post-meal using standard venepuncture techniques and divided between both serum and plasma (EDTA) vacutainers. Within 30 minutes of collection, samples were centrifuged for 12 mins at 4000 rpm, pipetted into 1 ml Eppendorf tubes and immediately frozen at  $-80^\circ\text{C}$ . Plasma lipids (total cholesterol, triglycerides, HDL cholesterol, and direct LDL cholesterol), liver function tests (ALT, AST, and GGT), Apolipoprotein A1 and B, C-reactive protein, and glucose were measured using an automated analyser (c311, Roche Diagnostics, Burgess Hill, UK). Insulin was also measured using an automated immunoassay analyser (e411, Roche Diagnostics, Burgess Hill, UK), while adiponectin, leptin and IL-6 (high sensitivity) were measured by ELISA (R&D systems, Abingdon, UK). All measures were made using the manufacturer's calibrators and quality control materials. Serum paraoxonase (PON-1) activities were measured by UV spectrophotometry in a 96-well plate format using paraoxon (SigmaAldrich, St Louis, Missouri). Metabolomic profiling was also performed on EDTA plasma samples by Nightingale Health (Finland) using a quantitative high-throughput NMR metabolomics platform, full details of which have been published elsewhere<sup>10</sup>.

#### Dataset 6 – psychological questionnaires

Three questionnaire-based psychological assessments were provided to participants on the day of testing in order to gauge indices of interpersonal support, happiness, and depression. The Interpersonal Support Evaluation List is a 12-item scale made up of three subscales – namely Tangible Support, Belonging Support, and Appraisal Support. All answers are given on a 4-point scale ranging from 'Definitely True' to 'Definitely False' and participants are required to rate each statement depending on its relevance to them. For analysis, the scores for negatively phrased statements are reversed and the scale totals for each subscale and the overall total are calculated<sup>10</sup>. The Oxford Happiness Questionnaire (OHQ) is a 29-item questionnaire; with each statement answered using a uniform 6-point Likert Scale. For analysis, negatively phrased questions are reversed and the sum total is divided by the number of questions to give an average score<sup>11</sup>. The Beck Depression Inventory II is a 21-question multiple choice self-report inventory used to assess the severity of depression. Questions are scaled from 0–3, with overall scores of 0–13 suggesting minimal depression,

14–19 mild depression, 20–28 moderate depression, and 29–63 severe depression<sup>12</sup>.

### Ethical approval and consent

Ethical approval for the study was obtained from the ALSPAC Ethics and Law Committee and the Local Research Ethics Committees. Full details of the approvals obtained are available from the study website (<http://www.bristol.ac.uk/alspac/researchers/research-ethics/>). Written informed consent was obtained from participants prior to their clinic visit. Study members have the right to withdraw their consent for elements of the study or from the study entirely at any time.

### Data

For ease of navigation, results include only variables that are deemed to be of particular relevance to this study and have

been separated into six distinct datasets contained within tables, namely **Table 1**, genetic risk groups; **Table 2**, participant characteristics; **Table 3**, adipose phenotypes; **Table 4**, cardiovascular phenotypes; **Table 5**, metabolic/metabolomic phenotypes; and **Table 6**, psychological questionnaires. A selection of example graphs showing relationships between BMI and a number of these adipose, vascular, cardiac, and metabolic phenotypes can be found in the extended data<sup>8</sup>.

**Table 1. Genetic risk groups dataset.**

Variable	Database ID	n	Mean (SD) or %
Genetic Risk Group (H/L)	Genetic Group	419	54/46

**Table 2. Participant characteristics dataset.**

Variable	Database ID	n	Mean (SD) or %
Age in years	Age	436	21.0 (1.0)
Participant sex (M/F)	Gender	436	34/66
Height in m	Ht	436	1.71 (0.09)
Weight in kg	Wt	436	72.2 (19.0)
Body mass index in kg/m <sup>2</sup>	Bmi	436	24.6 (5.7)
Waist circumference measured in cm	Waistcirm	435	82.5 (13.7)
Hip circumference measured in cm	Hipcirm	435	101.8 (11.5)
Sagittal-abdominal diameter measured in cm	Sad	435	15.9 (48.9)

**Table 3. Adipose phenotypes dataset.**

Variable	Database ID	n	Mean (SD)
Sum of visceral fat	Sumvf	409	20669 (20678)
Sum of subcutaneous fat	Sumsq	409	177688 (95361)
Sum of body volume	Sumbv	409	465622 (134155)
Number of voxels visceral fat	Vfvoxel	409	2091 (2525)
Number of voxels subcutaneous fat	Sqvoxel	411	17260 (9369)
Number of voxels total fat	Tfvoxel	409	19362 (10778)
Number of voxels body volume	Bvvoxel	409	43526 (15184)
Total body fat indexed to body volume	Tfibv	409	0.384 (0.154)
Visceral fat indexed to body volume	Vfibv	409	0.043 (0.036)
Subcutaneous fat indexed to body volume	Sqibv	409	0.415 (0.198)
Total fat indexed to body surface area	Tfbsa	409	10357 (4769)
Visceral fat indexed to body surface area	Vfbsa	409	1089 (1147)
Subcutaneous fat indexed to body surface area	Sqbsa	409	9310 (4189)
Subcutaneous fat indexed to visceral ratio	Sqrvf	409	12.2 (7.9)
Mean absolute liver fat	Livermean	412	184 (97)
Mean % liver fat	Liverfatperc	412	4.5 (2.4)
Pericardial fat volume	Pericardialvol	412	470 (411)

**Table 4. Cardiovascular phenotypes dataset.**

Variable	Database ID	n	Mean (SD)
<b>Carotid Intima-Media Thickness</b>			
Mean right carotid artery diameter measured during diastole in mm	Rblcdc123	434	6.21 (0.47)
Mean right carotid artery diameter measured during peak systole in mm	Rpkcdc123	434	7.06 (0.53)
Mean right carotid artery far-wall IMT measured during diastole in mm	Rblimt123	435	0.46 (0.05)
Mean right carotid artery far-wall IMT measured during peak-systole in mm	Rpkimt123	433	0.44 (0.05)
Mean left carotid artery diameter measured during diastole in mm	Lblcdc123	435	6.25 (0.48)
Mean left carotid artery diameter measured during peak systole in mm	Lpkcdc123	435	7.04 (0.51)
Mean left carotid artery far-wall IMT measured during diastole in mm	Lblimt123	435	0.46 (0.05)
Mean left carotid artery far-wall IMT measured during peak-systole in mm	Lpkimt123	432	0.45 (0.05)
<b>Pulse Wave Velocity</b>			
Carotid-Radial PWV in m/s	Pwvrad	434	6.79 (0.93)
Carotid-Femoral PWV when distance measured via umbilicus in m/s	Pwvfemviaub	419	5.59 (0.74)
Carotid-Femoral PWV when distance measured direct in m/s	Pwvfemdirect	418	5.37 (0.70)
<b>Flow-Mediated Dilatation</b>			
Baseline brachial artery diameter in mm prior to cuff inflation	Bldfmd	420	3.22 (0.52)
Peak percentage increase in arterial diameter following cuff deflation	Pkfmddperc	418	8.2 (4.0)
Time in seconds (from start of baseline) to reach peak percentage increase in arterial diameter following cuff deflation	Pkfmddtime	415	411 (17)
Mean baseline velocity-time integral in centimetres calculated from measurements 50, 30 and 10 seconds prior to cuff inflation	Blvti123	427	0.07 (0.03)
Peak velocity-time integral in centimetres measured following cuff deflation	Pkvti01	411	0.39 (0.11)
<b>Peripheral Blood Pressure</b>			
Systolic blood pressure measured immediately prior to PWA using brachial cuff occlusion in mmHg	Sbppwa	431	117 (10)
Diastolic blood pressure measured immediately prior to PWA using brachial cuff occlusion in mmHg	Dbppwa	431	67 (7)
Pulse pressure calculated immediately prior to PWA as systolic blood pressure – diastolic blood pressure	Pppwa	431	50 (10)
Mean arterial pressure calculated immediately prior to PWA as diastolic blood pressure + 1/3 (systolic blood pressure – diastolic blood pressure)	Mappwa	431	84 (7)
<b>Pulse Wave Analysis</b>			
Augmentation Pressure – extent to which central systolic pressure is augmented by the returning reflected pressure wave in mmHg	Augment	430	-0.51 (3.49)
Augmentation index (expressed as a percentage) calculated by dividing augmentation pressure by pulse pressure	Aiappp	430	-1.88 (10.38)
Augmentation index (expressed as a percentage) calculated by dividing pressure of the second peak observed within the central pressure waveform by the pressure of the first peak	Aip2p1	430	98.34 (11.14)

Variable	Database ID	n	Mean (SD)
Aortic systolic blood pressure estimated by PWA in mmHg	Pwaasp	430	98 (8)
Aortic diastolic blood pressure estimated by PWA in mmHg	Pwaadp	430	68 (7)
Aortic pulse pressure estimated by PWA in mmHg	Pwaapp	430	30 (6)
<b>Autonomic Function</b>			
BRS slope	Brsslope	365	20.3 (9.6)
Time Domain Heart rate variability, SDNN	Brstdhrv	357	73.3 (32.7)
Time Domain Heart rate variability, RMSSD	Brstdhrv2	357	68.9 (45.8)
Time Domain Heart rate variability, Triangular Index	Brstdhrv3	357	17.4 (6.1)
<b>Ultra-High Frequency Ultrasound</b>			
50 MHz right radial artery diameter measured in mm	vhrrrad50mhz	175	1.86 (0.39)
50 MHz right radial artery intima-media thickness measured in mm	vhrrraimt50mhz	175	0.15 (0.03)
50 MHz right radial artery intima thickness measured in mm	vhrrrait50mhz	175	0.07 (0.01)
50 MHz right radial artery media thickness measured in mm	vhrrramt50mhz	175	0.09 (0.03)
50 MHz right dorsal paedal artery diameter measured in mm	vhrrsdpad50mhz	145	1.31 (0.44)
50 MHz right dorsal paedal artery intima-media thickness measured in mm	vhrrsdpaimt50mhz	145	0.17 (0.11)
50 MHz right dorsal paedal artery intima thickness measured in mm	vhrrsdpait50mhz	145	0.07 (0.07)
50 MHz right dorsal paedal artery media thickness measured in mm	vhrrsdpamt50mhz	145	0.10 (0.06)
<b>Haemodynamic MRI Measures</b>			
Stroke volume in millilitres	Mriao1sv	387	90 (17)
Cardiac output in litres	Mriao1co	387	5.7 (1.2)
Systemic vascular resistance in mmHg/L/min	Mriao1svr	387	15.6 (3.0)
Total arterial compliance in ml/mmHg	Mriao1tac	387	1.02 (0.22)
<b>Cardiac Structure MRI Measures</b>			
Left ventricular end diastolic volume in millilitres	Mrilvedv	387	135 (27)
Left ventricular end systolic volume in millilitres	Mrilvesv	387	46 (14)
Left ventricular stroke volume in millilitres	Mrilvsv	387	89 (17)
Left ventricular ejection fraction (%)	Mrilvef	387	66 (5)
Left ventricular mass	Mrilvmas	387	91 (25)

**Table 5. Metabolic/metabolomic phenotypes.**

Variable	Database ID	n	Mean (SD)
Apolipoprotein B measured in g/L	ApoBgL	387	0.69 (0.23)
Apolipoprotein A measured in g/L	ApoAgL	387	1.16 (0.29)
C-reactive protein measured in mg/L	CRPmgL	366	2.00 (3.21)
Adiponectin measured in µg/L	Adiponectinugml	386	27.1 (16.3)
Leptin measured in ng/mL	Leptinngml	387	38.8 (36.2)
Interleukin-6 measured in pg/mL	IL-6pgml	375	1.45 (1.23)
Glucose measured in mmol/L	GlucosemmolL	385	3.75 (0.59)
Insulin measured in µU/mL	InsulinuUml	385	8.9 (6.2)
Gamma-glutamyl transferase measured in U/L	Ggtul	384	15.0 (14.8)
Alanine aminotransferase measured in U/L	Altul	385	17.0 (11.6)
Aspartate aminotransferase measured in U/L	Astul	384	24.8 (10.9)
Triglycerides measured in mmol/L	TRIGmmolL	384	0.73 (0.32)
Total cholesterol measured in mmol/L	CHOLmmolL	385	3.35 (1.01)
Low-density lipoprotein measured in mmol/L	LDLmmolL	384	1.85 (0.73)
High-density lipoprotein measured in mmol/L	HDLmmolL	384	1.03 (0.35)
Paraoxonase-1 Activity in µMol/P-Nitrophenol/L/Serum/min	PONActivityuMolPNitrophenol	304	877 (442)
Metabolomics	See <a href="#">extended data</a> <sup>8</sup> for complete list of all 225 biomarkers measured using NMR	228-389	-

**Table 6. Psychological questionnaires.**

Variable	Database ID	n
<b>Interpersonal Support Evaluation List</b>		
ISEL questions 1 – 12 as scored by participants	IseIq1 – IseIq12	224
Scaled and reversed totals of questions 1 – 12	IseIscttl1 – IseIscttl12	224
Appraisal subscale – calculated from total combined score of questions 2, 4, 6 and 11.	IseIappsubs	224
Belonging subscale – calculated from total combined score of questions 1, 5, 7 and 9.	IseIbelsubsc	224
Tangible subscale – calculated from total combined score of questions 3, 8, 10 and 12.	IseItangsubs	224
<b>Oxford Happiness Questionnaire</b>		
OHQ questions 1 – 29 as score by participants	Oxhqa1 – Oxhqa29	224
Converted totals for negatively phrased questions	Oxhct1 – Oxhct29	224
Sum of converted totals	Oxhsumct	224
Final score	Oxhscore	224
<b>Beck Depression Inventory II</b>		
BDI-II questions 1 – 21 as scored by participant	Prsonqa1 – Prsonqa21	224
Final Score	Prsonscore	224

## Dataset validation

In order to minimise variability inherent in the assessment of certain vascular phenotypes (e.g. carotid intima-media thickness, pulse-wave velocity, flow-mediated dilation), all study technicians working on the study were required to undergo identical training and accreditation procedures as those conducted in previous ALSPAC vascular clinics prior to scanning participants, details of which have been published elsewhere<sup>13,14</sup>. All blood samples were analysed in a single batch upon completion of the study in order to minimise any potential inter-assay variability. As with all large-scale studies, a number of variables have different degrees of missing data. Information on the extent of missing data for each variable can be found within each of the descriptive tables provided within this data note. Of note, around 10% of participants refused to provide a blood sample due to fear of needles. In addition, ultra-high frequency resolution ultrasound and psychological questionnaires were only added to the main study protocol in 2013, and data for these variables are therefore available in only a sub-sample of participants.

## Data availability

### Underlying data

ALSPAC data access is through a system of managed open access. Full details of all available data can be accessed through a fully searchable data dictionary provided on the ALSPAC study website (<http://www.bris.ac.uk/alspac/researchers/data-access/data-dictionary>) and the steps below highlight how to apply for access to both the data included in this data note and all other ALSPAC data. The datasets presented in this data note are linked to ALSPAC project number B645; please quote this project number during your application. The ALSPAC variable codes highlighted in the dataset descriptions can be used to specify required variables.

1. Please read the [ALSPAC access policy \(PDF, 627kB\)](#) which describes the process of accessing the data and samples in detail and outlines the costs associated with doing so.
2. You may also find it useful to browse our fully searchable [research proposals database](#), which lists all research projects that have been approved since April 2011.
3. Please [submit your research proposal](#) for consideration by the ALSPAC Executive Committee using the online process. You will receive a response within 10 working days to advise you whether your proposal has been approved.

If you have any questions about accessing data, please email [alspac-data@bristol.ac.uk](mailto:alspac-data@bristol.ac.uk).

The ALSPAC data management plan describes in detail the policy regarding data sharing, which is through a system of managed open access.

### Extended data

Extended data, including example graphs showing relationships between BMI and other phenotypes, descriptive metabolomics data and the ALSPAC in London medical history questionnaire, can be found in the figshare data repository. DOI: <https://doi.org/10.6084/m9.figshare.c.4337849.v1><sup>8</sup>.

Data are available under the terms of the [Creative Commons Zero “No rights reserved” data waiver](#) (CC0 1.0 Public domain dedication).

### Grant information

This publication is the work of the authors and STC will serve as guarantor for the contents of this paper. The UK Medical Research Council and Wellcome Trust (Grant ref: 102215/2/13/2) and the University of Bristol provide core support for ALSPAC. This research was specifically funded by the British Heart Foundation (BHF Programme Grant No. RG/10/004/28240). JED was a BHF-funded Professor during the time of this study. NJT is a Wellcome Trust Investigator (202802/Z/16/Z), is the PI of the Avon Longitudinal Study of Parents and Children (MRC & WT 102215/2/13/2), is supported by the University of Bristol NIHR Biomedical Research Centre (BRC-1215-20011), the MRC Integrative Epidemiology Unit (MC\_UU\_12013/3) and works within the CRUK Integrative Cancer Epidemiology Programme (C18281/A19169). KHW was supported by a Wellcome Trust Grant (096989/Z/11/Z). A comprehensive list of grants funding is available on the ALSPAC website.

*The funders had no role in study design, data collection and analysis, decision to publish, or preparation of the manuscript.*

### Acknowledgements

We are extremely grateful to all the families who took part in this study, the midwives for their help in recruiting them, and the whole ALSPAC team, which includes interviewers, computer and laboratory technicians, clerical workers, research scientists, volunteers, managers, receptionists and nurses.

## References

1. Corbin LJ, Tan VY, Hughes DA, *et al.*: **Formalising recall by genotype as an efficient approach to detailed phenotyping and causal inference.** *Nat Commun.* 2018; 9(1): 711. [PubMed Abstract](#) | [Publisher Full Text](#) | [Free Full Text](#)
2. Fraser A, Macdonald-Wallis C, Tilling K, *et al.*: **Cohort Profile: the Avon Longitudinal Study of Parents and Children: ALSPAC mothers cohort.** *Int J Epidemiol.* 2013; 42(1): 97–110. [PubMed Abstract](#) | [Publisher Full Text](#) | [Free Full Text](#)
3. Boyd A, Golding J, Macleod J, *et al.*: **Cohort Profile: the ‘children of the 90s’—the index offspring of the Avon Longitudinal Study of Parents and Children.** *Int J Epidemiol.* 2013; 42(1): 111–27. [PubMed Abstract](#) | [Publisher Full Text](#) | [Free Full Text](#)

4. Speliotes EK, Willer CJ, Berndt SI, *et al.*: **Association analyses of 249,796 individuals reveal 18 new loci associated with body mass index.** *Nat Genet.* 2010; **42**(11): 937–48.  
[PubMed Abstract](#) | [Publisher Full Text](#) | [Free Full Text](#)
5. Stergiakouli E, Martin J, Hamshere ML, *et al.*: **Association between polygenic risk scores for attention-deficit hyperactivity disorder and educational and cognitive outcomes in the general population.** *Int J Epidemiol.* 2017; **46**(2): 421–8.  
[PubMed Abstract](#) | [Publisher Full Text](#) | [Free Full Text](#)
6. Stergiakouli E, Gaillard R, Tavaré JM, *et al.*: **Genome-wide association study of height-adjusted BMI in childhood identifies functional variant in *ADCY3*.** *Obesity (Silver Spring).* 2014; **22**(10): 2252–9.  
[PubMed Abstract](#) | [Publisher Full Text](#) | [Free Full Text](#)
7. McCarron P, Smith GD, Okasha M, *et al.*: **Blood pressure in young adulthood and mortality from cardiovascular disease.** *Lancet.* 2000; **355**(9213): 1430–1.  
[PubMed Abstract](#) | [Publisher Full Text](#)
8. Chiesa S, Rapala A, Charakida M, *et al.*: **The 'ALSPAC in London' dataset: adiposity, cardiometabolic risk profiles, and the emerging arterial phenotype in young adulthood.** *figshare.* Collection. 2018.
9. Bertinieri G, Di Rienzo M, Cavallazzi A, *et al.*: **Evaluation of baroreceptor reflex by blood pressure monitoring in unanesthetized cats.** *Am J Physiol.* 1988; **254**(2 Pt 2): H377–83.  
[PubMed Abstract](#) | [Publisher Full Text](#)
10. Cohen S, Hoberman HM: **Positive Events and Social Supports as Buffers of Life Change Stress1.** *J Appl Soc Psychol.* 1983; **13**(2): 99–125.  
[Publisher Full Text](#)
11. Hills P, Argyle M: **The Oxford Happiness Questionnaire: a compact scale for the measurement of psychological well-being.** *Pers Individ Dif.* 2002; **33**(7): 1073–82.  
[Publisher Full Text](#)
12. Beck AT, Ward CH, Mendelson M, *et al.*: **An inventory for measuring depression.** *Arch Gen Psychiatry.* 1961; **4**: 561–71.  
[PubMed Abstract](#) | [Publisher Full Text](#)
13. Charakida M, Jones A, Falaschetti E, *et al.*: **Childhood obesity and vascular phenotypes: a population study.** *J Am Coll Cardiol.* 2012; **60**(25): 2643–50.  
[PubMed Abstract](#) | [Publisher Full Text](#)
14. Donald AE, Charakida M, Falaschetti E, *et al.*: **Determinants of vascular phenotype in a large childhood population: the Avon Longitudinal Study of Parents and Children (ALSPAC).** *Eur Heart J.* 2010; **31**(12): 1502–10.  
[PubMed Abstract](#) | [Publisher Full Text](#) | [Free Full Text](#)